ISSN 0965-545X, Polymer Science, Ser. A, 2015, Vol. 57, No. 4, pp. 445–451. © Pleiades Publishing, Ltd., 2015.
Original Russian Text © A.E. Chalykh, U.V. Nikulova, A.A. Shcherbina, 2015, published in Vysokomolekulyarnye Soedineniya. Ser. A, 2015, Vol. 57, No. 4, pp. 346–353.

Phase Equilibria in a Polystyrene–Poly(butyl acrylate) System

A. E. Chalykh, U. V. Nikulova, and A. A. Shcherbina

Frumkin Institute of Physical Chemistry and Electrochemistry, Russian Academy of Sciences, Moscow, 119071 Russia

e-mail: aachalykh@mail.ru

Received December 11, 2014;
Revised Manuscript Received January 28, 2015

Abstract—Phase equilibria in polystyrene–poly(*n*-butyl acrylate) systems containing polystyrene of various molecular masses were studied for the first time via optical interferometry at temperatures between 280 and 500 K. The phase diagrams of the systems were obtained, the pair interaction parameters were determined, and the dependences of the parameters on the molecular mass of polystyrene and temperature were found. The possibility of thermodynamic analysis of phase diagrams in terms of the classical Flory–Huggins–Scott theory and the possibility to predict generalized phase diagrams of polystyrene–poly(*n*-butyl acrylate) systems on the basis of the experimental values of the pair interaction parameters were shown.

DOI: 10.1134/S0965545X15040069

In recent years, in the field of polymer chemistry, the controlled synthesis of copolymers of a given architecture of the macromolecular chain has been actively investigated. In particular, copolymers of homogeneous compositions and various structures with a narrow molecular-mass distribution—including multiblock, gradient, and random copolymers—have been studied [1–3]. However, in addition to the features of the method used to prepare copolymers [4–6], the data on the intermolecular interaction of the initial homopolymers of the copolymers are of great importance to estimate the properties of the copolymers and the characteristics of their supramolecular organization [7, 8]. In [9–12], an independent study of the solubilities, thermodynamics of mixing, and phase structures of mixtures of homopolymers was reported to be necessary to obtain the above-mentioned data.

Poly(*n*-butyl acrylate) (PBA) and polystyrene (PS) are one of the pairs of polymers used in the design of pressure-sensitive adhesives [13] and adhesives for various purposes [14] as well as in the synthesis of copolymers with various microstructures of chains [3, 5, 15, 16]. Until recently, these polymers were thought to be completely incompatible [17]. However, this conclusion was drawn based on the determination of the solubilities of melts and solutions of polymers characterized by $M \gg 10^5$. For example, the limit of compatibility of PS with $M = 5.2 \times 10^5$ and PBA with $M = 1.19 \times 10^5$ was found in [18, 19] via the melt-titration technique at a temperature of 423 K to be ~0.001 wt %. In continuation of these studies, the goal of the present study was to extend the range of measurements and examine in detail the phase equilibrium in the PBA–PS system within a wide range of temperatures and molecular masses of the components.

EXPERIMENTAL

PBA and PS with narrow molecular-mass distributions (Sigma-Aldrich) were used. Their characteristics are summarized in Table 1.

The solubilities of polymers were examined via the laser interference microscopy method [20, 21]. PS films 120–150 μm thick prepared via the pressing technique were used in all measurements.

A convenient measurement technique [22] was used. PS film samples 5 mm × 10 mm in area were placed between two 5-mm-thick pieces of optically transparent glass with a semitransparent layer of metal (nichrome) characterized by a high coefficient of reflection applied on their inner surfaces via thermal vacuum deposition. A small wedge angle of approximately 5° was formed by metal fixators of various thicknesses (for example, 100 and 120 μm for a 120-μm-thick PS film). The samples were brought into optical contact with the inner surfaces of the pieces of glass at a temperature 20–30 K higher than the glass-transition temperature of PS, with the largest

Table 1. Characteristics of the studied polymers

Polymer	$M_n \times 10^{-3}$	M_n/M_w	T_g^*, K	T_{degr}^*, K
PBA	35.0	1.17	223	570
PS-1	1.2	1.03	343	550
PS-2	2.3	1.07	348	550
PS-3	3.6	1.01	353	550
PS-4	4.1	1.00	353	550
PS-5	30.0	1.02	373	566

*Obtained from DSC and TGA data.

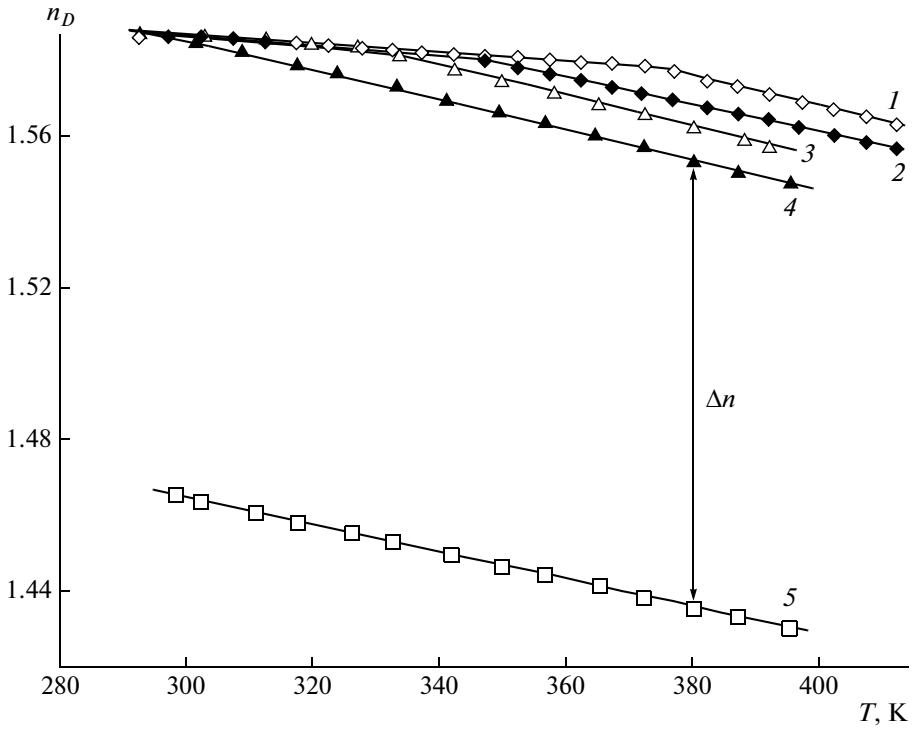

Fig. 1. Temperature dependences of the refractive indexes of (*1*) PS-5, (*2*) PS-3, (*3*) PS-2, (*4*) PS-1, and (*5*) PBA.

side of the sample being placed perpendicularly to the edge of wedge. In this case, the direction of the diffusion flux coincided with that of the interference bands. The formed cell was placed into a diffusion cell at a temperature controlled with a precision of ±1 K. A capillary was then filled with the melt of PBA, and the moment of the contact of PS phase with PBA phase was considered to be the beginning of the diffusion process.

A helium–neon laser with a wavelength of 632 nm was used as a light source. The interference patterns were recorded with the use of a digital video camera, and the images were transferred to a personal computer. Measurements were taken in the regime of stepwise increases and decreases in temperature from 280 to 500 K. The interference patterns were processed via a convenient technique [21, 22].

The temperature dependences of the refractive indexes of PS and PBA were obtained in the preliminary experiments (Fig. 1). At temperatures above T_g, for example, at 380 K for PS-1, the difference between the refractive indexes of PS and PBA was shown to be 0.13 and corresponded to the appearance of approximately 42 interference bands in the interdiffusion zone. This result indicates that the increment of the refractive index per band is 0.003 and that the precision of measurement of the concentration change between two bands is 2.4 vol %.

RESULTS AND DISCUSSION

Interdiffusion Zones

Figure 2 shows typical interference patterns of the regions of conjugation of phases, that is, interdiffusion zones between PBA and PS. At temperatures from 363 to 433 K, the interdiffusion zone of samples of PS with $M_n \geq 3.6 \times 10^3$ is the superposition of three regions: namely, the regions of pure PS and PBA, **I** and **II**, respectively; the phase boundary, **V**; the region of dissolution of PBA in PS, **IV**; and the region of dissolution of PS in PBA, **III**.

Under the used isothermal conditions, the concentrations corresponding to the compositions of coexisting phases, φ' and φ", that is, the limit solubilities of PBA in PS and PS in PBA at a given temperature, are established on both sides of the phase boundary and remain constant during the whole observation period. The compositions of the coexisting phases at the phase boundary were determined according to the technique used in [23] for the treatment of concentration profiles. This structure of the transition zone characterized by a concentration gradient is general and observed in all studied PS–PBA systems. The specificities of the various systems consist in the various extensions of interdiffusion zones and the various numerical values of the compositions of the coexisting phases.

In regions **III** and **IV** of the mixing of components, in contrast to phase boundary **V**, the continuous changes in both the sizes of regions and the profiles of

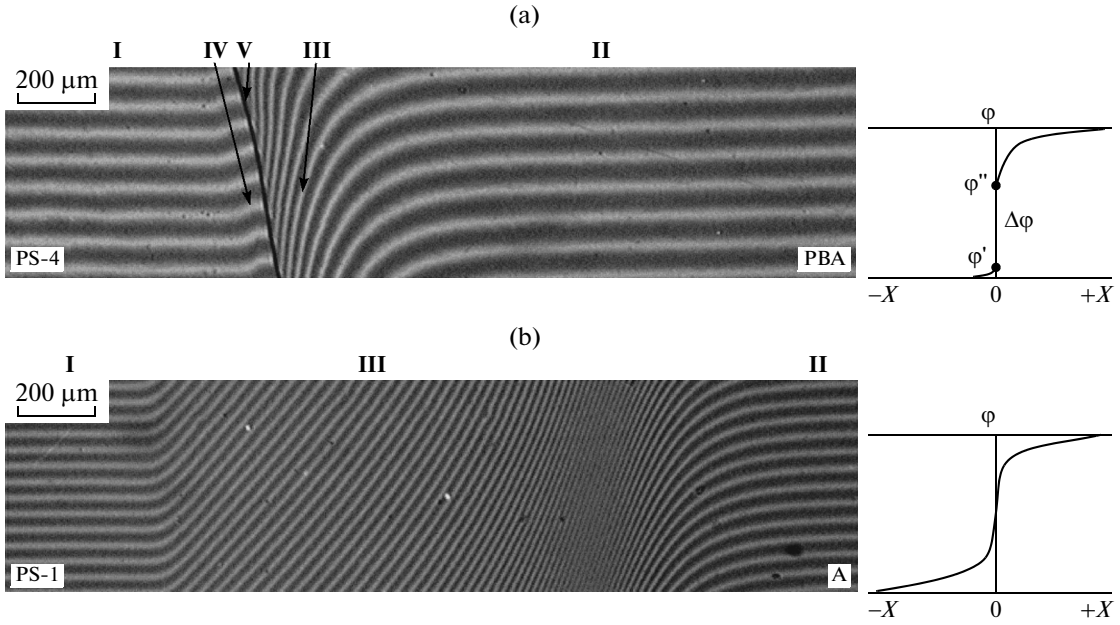

Fig. 2. Interference patterns (left) and corresponding schematic profiles of the concentration distribution (right) characterizing the interdiffusion zones of PBA and (a) PS-4 at 443 K or (b) PS-1 at 403 K.

the concentration distribution of components within the regions with time are observed. All points of the concentration profiles change their positions along the X diffusion coordinate strictly according to the $X - t^{1/2}$ law of diffusion (Fig. 3); that is, the diffusion mechanism of mixing of polymers is observed.

An increase in temperature leads to the convergence of compositions of coexisting phases toward each other at the phase boundary, thereby resulting in degradation of the boundary at the mixing temperature. Under these conditions, the interdiffusion zone consists of interference bands smoothly varying after the transition from one pure component to the other (Fig. 2b, region **III**). That is, a single-phase gradient structure is formed.

The subsequent step cooling leads to the appearance of the phase boundary within the interdiffusion zone, and the regions of amorphous separation spontaneously form near the boundary. These regions are located in a certain area of the concentration profile at a given temperature. During long-term observation at T = const, the following stages occur: the formation of local matrix-inclusion dispersed structures in the mentioned zones, complete separation of these structures via the Ostwald maturation mechanism, and the final formation of the above-described structure of the interdiffusion zone after heating.

Note that the complete mutual dissolution of the components of systems containing PS with $M_n \geq 3 \times 10^3$ is not observed up to the decomposition temperatures of the components (Table 1). In this case, the zone of dissolution of PS in PBA that increases with temperature is observed only (Fig. 2a, region **III**). The limit of solubility of PBA in the PS matrix (Fig. 2a, region **IV**) does not exceed ~5 vol %, even at high temperatures.

Phase Diagrams

Binodal curves of the diagrams of amorphous separation of PS–PBA systems were plotted at various

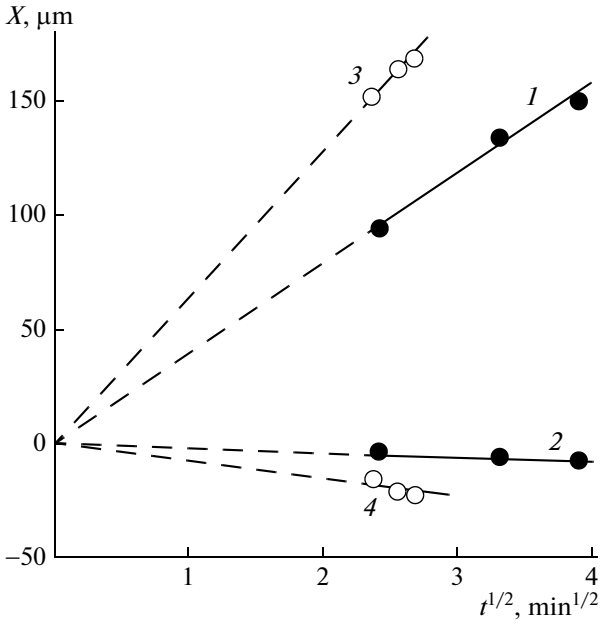

Fig. 3. Kinetics of motion of the diffusion front of (*1*, *3*) PS in PBA and (*2*, *4*) PBA in PS measured at (*1*, *2*) 413 K and (*3*, *4*) 423 K.

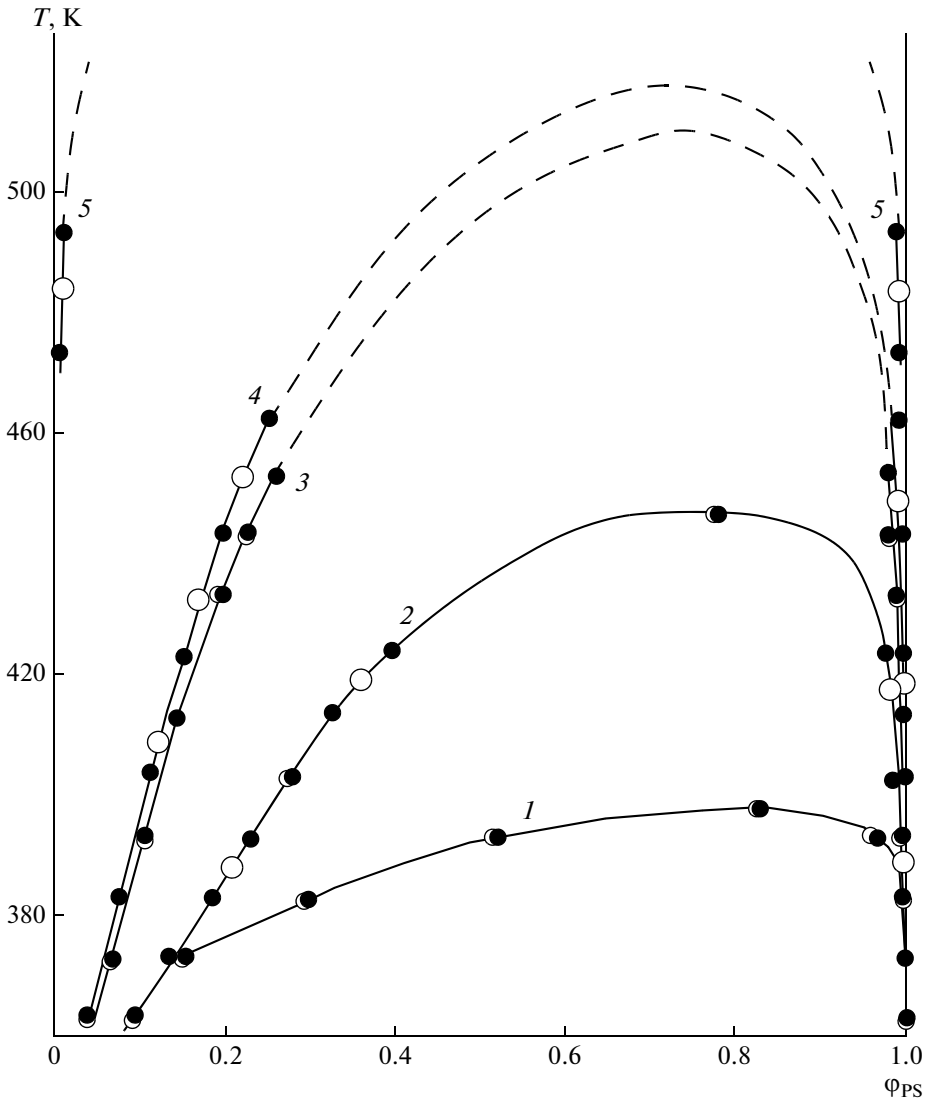

Fig. 4. Phase diagrams of PBA–PS systems containing (*1*) PS-1, (*2*) PS-2, (*3*) PS-3, (*4*) PS-4, and (*5*) PS-5. Experimental data were obtained during (black circles) heating and (white circles) cooling, and (dashed lines) the binodal domes of curves *3* and *4* were calculated with the use of the program PhaDiag.

temperatures on the basis of the compositions of coexisting phases (Fig. 4). Analysis of these dependences makes it possible to make the following conclusions. First, the data on the compositions of coexisting phases obtained after step heating agree well with those obtained after step cooling, a result that suggests the reproducibility and equilibrium of the boundary curves. Second, in all cases, the solubilities of polymers increase with an increase in temperature. This circumstance indicates the presence of the upper critical solution temperature (UCST) in the studied systems. The UCST was experimentally determined only in the case of PS with $M_n < 3 \times 10^3$ (Fig. 4). Third, the positions of the binodal domes depend on the molecular mass of PS. Systems containing oligomeric PSs—PS-1 and PS-2—show complete solubility at temperatures above 403 and 443 K, respectively. For other systems, the binodal domes are located in the region of high temperatures close to the region of thermal degradation of polymers (Fig. 4, Table 1).

The thermodynamic analysis of the experimental data was performed under the following assumptions. The following relationships exist between the chemical potentials of components for all compositions of coexisting phases of binodal curves:

$$\Delta\mu_1' = \Delta\mu_1'' \quad \text{and} \quad \Delta\mu_2' = \Delta\mu_2'',$$

where $\Delta\mu_i$ is the change in the chemical potential of the ith component in the first ($\Delta\mu_i'$) and second ($\Delta\mu_i''$) phases.

Expressions for the chemical potentials of components are derived from the Flory–Huggins–Scott theory of polymer solutions [24] with allowance for the

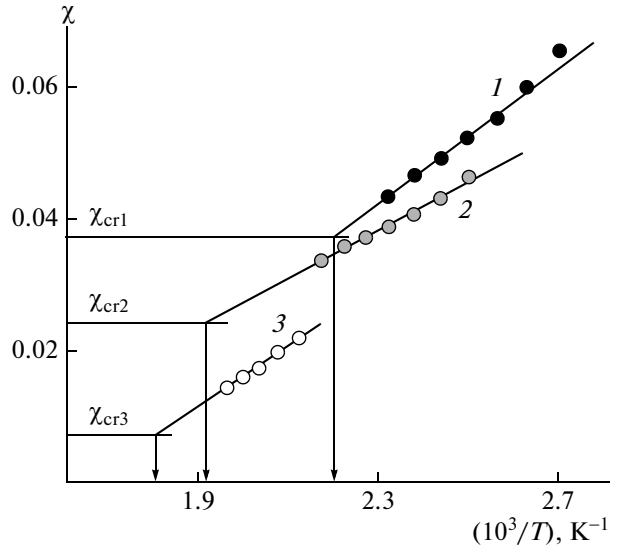

Fig. 5. Temperature dependences of the pair interaction parameters for PBA and (*1*) PS-2, (*2*) PS-4, and (*3*) PS-5 with arrows indicating the UCST positions.

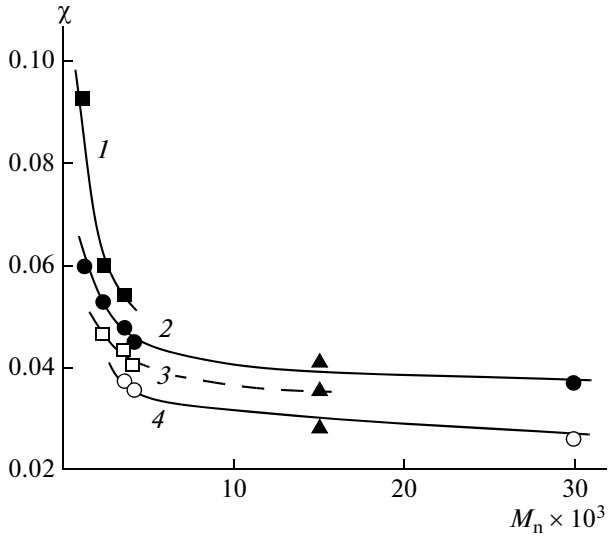

Fig. 6. Dependences of the pair interaction parameter of PBA and PS on the molecular mass of PS at (*1*) 380, (*2*) 400, (*3*) 420, and (*4*) 450 K with triangles indicating points calculated via the proposed technique for a PS with $M_n = 1.5 \times 10^4$.

concentration dependence of the pair interaction parameter, $\chi(\varphi_i)$):

$$\ln \varphi_1' + \left(1 - \frac{r_1}{r_2}\right)\varphi_2' + r_1\chi_{12}(\varphi_2')^2 = \ln \varphi_1'' + \left(1 - \frac{r_1}{r_2}\right)\varphi_2'' + r_1\chi_{12}(\varphi_2'')^2 \quad (1)$$

$$\ln \varphi_2' + \left(1 - \frac{r_2}{r_1}\right)\varphi_1' + r_2\chi_{21}(\varphi_1')^2 = \ln \varphi_2'' + \left(1 - \frac{r_2}{r_1}\right)\varphi_1'' + r_2\chi_{21}(\varphi_1'')^2 \quad (2)$$

where r_i is the degree of polymerization of a component, φ_i' is the volume fraction of the ith component in the first phase, φ_i'' is the volume fraction of the ith component in the second phase, $\chi_{12} = \chi + \frac{\partial\chi}{\partial\varphi_1}$, $\chi_{21} = \chi + \frac{\partial\chi}{\partial\varphi_2}$, and χ is the pair interaction parameter.

Table 2. Thermodynamic characteristics of systems at the critical point

PS	$M_n \times 10^{-3}$	χ_{crit} (calculated)	T_{crit}, K
1	1.2	0.063	403/397*
2	2.3	0.037	443/446*
3	3.6	0.027	510*
4	4.1	0.024	523*
5	30.0	0.007	559*

* Values calculated via the described technique.

The solutions to Eqs. (1) and (2) with respect to χ_{12} and χ_{21} lead to the following equations:

$$\chi_{12} = \frac{\ln \varphi_1'' - \ln \varphi_1'}{r_1((\varphi_2')^2 - (\varphi_2'')^2)} - \left(\frac{1}{r_1} - \frac{1}{r_2}\right)\frac{1}{\varphi_2' + \varphi_2''}, \quad (3)$$

$$\chi_{21} = \frac{\ln \varphi_2'' - \ln \varphi_2'}{r_2((\varphi_1')^2 - (\varphi_1'')^2)} - \left(\frac{1}{r_2} - \frac{1}{r_1}\right)\frac{1}{\varphi_1' + \varphi_1''}. \quad (4)$$

The parameters of the critical point are determined by the following equation [23]:

$$\chi_{cr} = \frac{1}{2}\left(\frac{1}{\sqrt{r_1}} + \frac{1}{\sqrt{r_2}}\right)^2. \quad (5)$$

The numerical χ_{12} and χ_{21} values of the PS–PBA system were calculated through Eqs. (3) and (4) on the basis of the composition of the coexisting phases. Note that the obtained χ_{12} and χ_{21} values actually coincide. This result indicates the absence of the concentration dependence of the pair interaction parameters of the components in the system.

The temperature dependences of χ are shown in Fig. 5. The values of the pair interaction parameter change within the relatively narrow range 0.01–0.07. All of the studied systems show linear dependences of χ on T^{-1}, with the extrapolation of the latter to the critical conditions (Eq. (5)) making it possible to estimate the UCST values. These values are close to those measured experimentally (Table 2). The slopes of the temperature dependences are positive, a circumstance that is typical of systems characterized by the presence of the UCST.

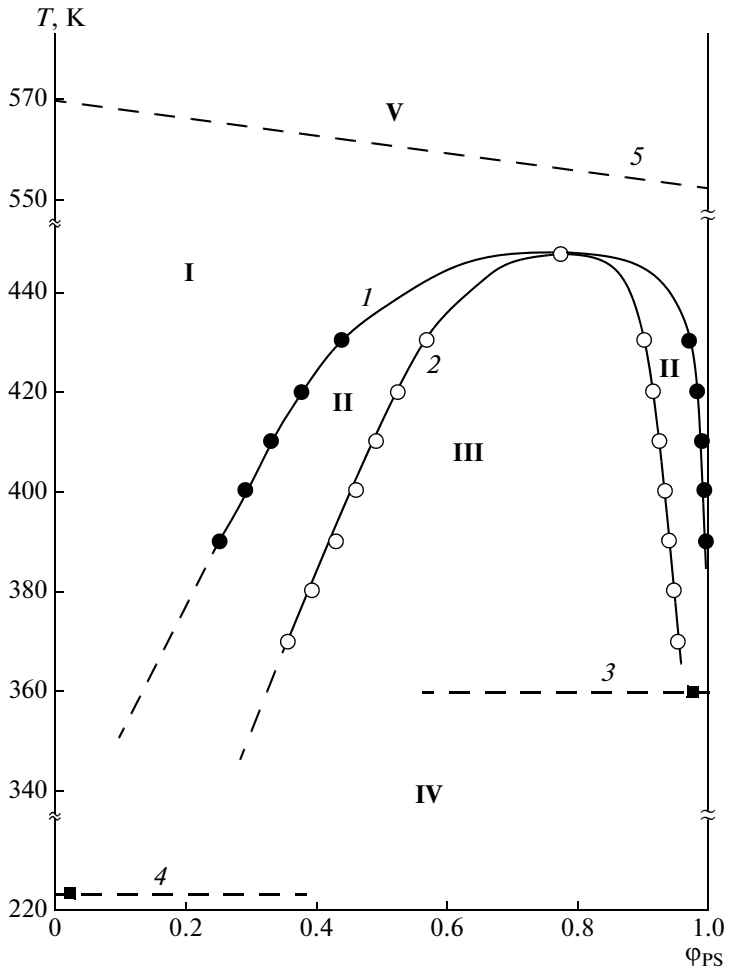

Fig. 7. Calculated generalized phase diagram of the PBA–PS-2 system with indicated (*1*) binodal and (*2*) spinodal positions of the T_g values of (*3*) PS and (*4*) PBA, and (*5*) the line of destruction of components.

The dependences of the pair interaction parameters on the molecular mass of PS at various temperatures are summarized in Fig. 6. Parameter χ decreases with an increase in the molecular mass of PS, asymptotically approaching the limit χ_∞ values of approximately 0.03 at 450 K and 0.04 at 400 K.

On the basis of the temperature dependences of χ, binodal and spinodal curves were calculated and generalized phase diagrams were obtained. The results suggest that the examined systems follow the classical Flory–Huggins–Scott theory. Figure 7 shows that the generalized diagram of the oligomeric PS-2–PBA system includes the critical point and the binodal and spinodal curves dividing the temperature and concentration field into the region of true solutions, **I**; the region of metastable states, **II**; and the region of labile solutions, **III**. In addition, the diagram contains data on the values of the glass-transition temperatures of PS and PBA; region **IV** of the vitrification of the components of the system; and boundary dashed line *5*, separating region **V** of the thermal degradation of polymers and their compositions.

In conclusion, it was shown that the phase behavior of PBA–PS systems may be predicted in a wide range of molecular masses of the components on the basis of the dependences of the pair interaction parameters on temperature and molecular mass. Therefore, the boundary curves of the diagrams of the phase and physical states of the previously studied PS–PBA system [18] containing polymers of high molecular masses (PS of $M = 5.2 \times 10^5$ and PBA of $M = 1.19 \times 10^5$) were calculated. Note that the dependence of χ on T^{-1} (Fig. 5) was used in all calculations after its extrapolation to the values at the critical point. The obtained diagrams (solid and dashed lines) and the literature data (point *2*) [18, 19] are shown in Fig. 8. The calculated binodal and spinodal curves are located in the region of infinitely dilute solutions. This result agrees well with the experimental data previously obtained in [18, 19].

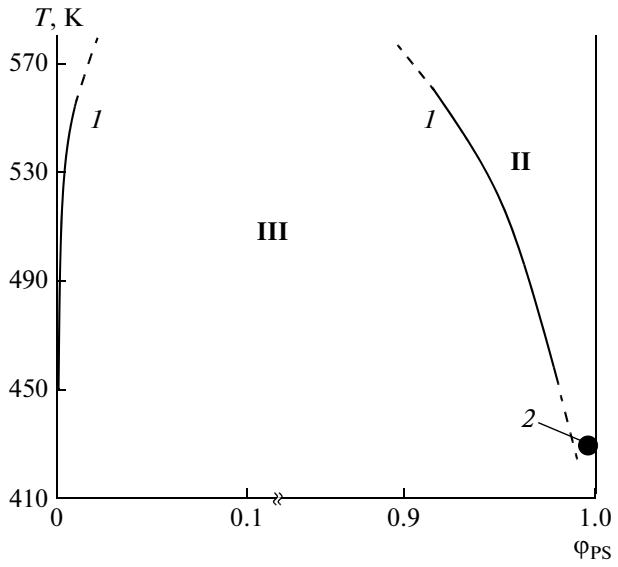

Fig. 8. (*1*) Calculated spinodal and (*2*) experimental data [18] for the PS–PBA system containing PS with $M = 5.2 \times 10^5$ and PBA with $M = 1.19 \times 10^5$. Regions **II** and **III** correspond to those in Fig. 7.

ACKNOWLEDGMENTS

The authors thank E.V. Chernikova for supplying a sample of PBA synthesized via pseudo-living RAFT-polymerization at the Department of Macromolecular Compounds of Moscow State University.

This work was financially supported by the Russian Foundation for Basic Research (project nos. 14-03-00142 and 14-03-00390).

REFERENCES

1. *Controlled and Living Polymerization: from Mechanisms to Applications*, Ed. A. H. E. Muller and K. Matyjaszewski (Wiley-VCH, Weinheim, 2009).
2. N. Hadjichristidis, S. Pispas, and G. Floudas, *Block Copolymers: Synthesis Strategies, Physical Properties, and Applications* (Wiley, Hoboken, 2003).
3. Y. Chong, T. P. Le, G. Moad, E. Rizzardo, S. H. Thang, Macromolecules **32** (6), 2071 (1999).
4. E. V. Chernikova, P. S. Terpugova, E. S. Garina, and V. B. Golubev, Polym. Sci., Ser. A **49** (2), 108 (2007).
5. E. V. Chernikova, P. S. Terpugova, M. Y. Trifilov, E. S. Garina, V. B. Golubev, E. V. Sivtsov, Polym. Sci., Ser. A **51** (6), 658 (2009).
6. E. V. Chernikova, A. V. Tarasenko, V. V. Yulusov, E. S. Garina, V. B. Golubev, Polym. Sci., Ser. A **51** (6), 667 (2009).
7. S. Krause, J. Polym. Sci., Part A: Polym. Chem. **7**, 249 (1969).
8. D. J. Dunn and S. Krause, J. Polym. Sci., Polym. Lett. Ed. **12**, 591 (1974).
9. A. E. Chalykh and V. K. Gerasimov, Russ. Chem. Rev. **73** (1), 59 (2004).
10. V. K. Gerasimov, Doctoral Dissertation in Chemistry (IFKhE RAN, Moscow, 2012).
11. V. N. Kuleznev, *Blends and Alloys of Polymers* (Nauchnye osnovy i tekhnologii, St. Petersburg, 2013) [in Russian].
12. U. V. Nikulova, A. E. Chalykh, and A. S. Nikulov, Izv. Vyssh. Uchebn. Zaved., Khim. Khim. Tekhnol. **51** (12), 28 (2008).
13. *Handbook of Pressure Sensitive Adhesive Technology*, Ed. by D. Satas (Satas&Associates, Warwick, Rhode Island, 1999).
14. L. M. Pritykin, D. A. Kardashov, and V. L. Vakula, *Monomer Adhesives* (Khimiya, Moscow, 1988) [in Russian].
15. A. E. Chalykh and A. A. Shcherbina, *Handbook of Pressure-Sensitive Adhesives and Products*, Ed. by I. Benedek and M. M. Feldstein (CRC Press Taylor&Francis Group, Boca Raton, FL, 2009).
16. A. A. Shcherbina, A. V. Shapagin, and E. V. Chernikova, in *Proceedings of the Sixths All-Russian Kargin Conference "Polimery-2014"*(Moscow, 2014), Vol. 3, p. 926 [in Russian].
17. S. Krause, in *Polymer Blends*, Ed. by D. R. Paul and S. Newman (Acad. Press, New York, London, 1978).
18. R. H. Somani and M. T. Shaw, Macromolecules **14**, 1549 (1981).
19. O. Olabisi, L. M. Robeson, and M. T. Shaw, *Polymer-Polymer Miscibility* (Acad. Press, New York, 1979).
20. A. Ya. Malkin and A. E. Chalykh, *Diffusion and Viscosity of Polymers: Measurement Techniques* (Khimiya, Moscow, 1979).
21. A. E. Chalykh, A. I. Zagaitov, V. V. Gromov, and D. P. Korotchenko, *Optical diffusiometer "ODA-2". Technical Guide* (IFKh RAN, Moscow, 1996) [in Russian].
22. A. E. Chalykh and U. V. Nikulova, Polym. Sci., Ser. A **53** (9), 811 (2011).
23. A. E. Chalykh, V. K. Gerasimov, and Yu. M. Mikhailov, *Diagrams of Phase State of Polymer Systems* (Yanus-K, Moscow, 1998) [in Russian].
24. *Multicomponent Polymer Systems*, Ed. by R. F. Gould (American Chemical Society, Washington, 1971).

Translated by D. Lonshakov